Measurement of liquid properties by the observation of micro droplet emitted by inkjet

T. Yamada* and K Sakai*

* Institute of industrial Science, University of Tokyo
Be305, Institute of Industrial Science, 4-6-1 Komaba, Meguro-ku, Tokyo, Japan
tyamada@iis.u-tokyo.ac.jp

ABSTRACT

Inkjet processes involve large shear deformation of liquid in microscale,which cannot be obtained by the conventional measurement techniques, such as viscometers and rheometers, dealing with millimeter-size liquid.

We introduce here the measurement of the liquid properties by observing the dynamic mechanical behavior of a 10-micron droplet. We observed the fundamental oscillation brought about by a head-on collision of two droplets, which gives us information on the surface tension and viscosity. We also observed equilibrium shapes of a combined droplet of immiscible liquids, and obtained surface and interfacial properties of the microscale liquid.

These experiments will provide fundamental knowledges on the behavior and properties of microscale liquids, and be useful for the inkjet application such as a manufacturing of the functional microparticles.

Keywords: inkjet, micro droplet, drop oscillation, surface tension, viscosity

1 INTRODUCTION

Inkjet printing technology is now widely applied to the industrial processes such as fabrication of organic electroluminescence display, wiring of a solar panel, and LED color filter. Recently, new application of the inkjet technology to the bioengineering has been in the spotlight.

Since these processes induce large shear deformation to the microscale liquid, the importance of the measurement of the micron liquid properties under high-shear flow is increasing, however, the conventional measurement techniques such as viscometers and rheometers can only deal with the millimeter-size liquid.

In the typical inkjet process, the radius of the droplet is in the order of 10-micron and the initial emission velocity is around 10 m/s, therefore, the characteristic shear flow rate almost reaches 10^6 s^{-1}. Such large shear deformation causes turbulent flow for macroscopic fluid. In contrast, the behavior of micron-size liquid is known to be stable by the following reason. The characteristic Reynolds number is defined as

$$Re = \rho U L/\eta, \tag{1}$$

where ρ, η are fluid density and viscosity, U and L are the characteristic velocity and length, respectively. If the characteristic shear flow rate is $U/L = 10^6$ s^{-1} and liquid viscosity is $\eta = 1$ mPa·s, the Reynolds number is in the order of 10^6 for $L = 1$ mm, while it is only 100 for $L = 10\mu$m. Obviously, the fluid motion is in turbulent flow in former case while it is stable laminar flow in the latter.

For the low Reynolds number flow, the motion of the liquid obeys the linearized Navier-Stokes equation of,

$$\rho\frac{d\mathbf{v}}{dt} = -\nabla p + \eta\nabla^2\mathbf{v}, \tag{2}$$

$\mathbf{v}$ and p being the fluid velocity and pressure. The incompressible condition of

$$\nabla\cdot\mathbf{v} = 0, \tag{3}$$

with the boundary condition expressed by Young-Laplace equation

$$\Delta p = -\sigma\nabla\cdot\mathbf{n} = 2\sigma H, \tag{4}$$

and σ and H being the surface/interfacial tension and the mean curvature of surface/interface, also hold for the microscopic process. From these equations we can obtain the viscosity and surface tension, by observing the mechanical behavior of microscale fluids.

Taking advantage of the low Reynolds number process of the microscale fluids, microfluidic devices are expected as the novel tool for the fabrication of the microfunctional materials. The stability of the system would provide products with high monodispersity, however, large viscous resistance would prevent mass production. We are recently studying a new application of inkjet to the fabrication process of the functional microparticles. Our newly developed inkjet equipment can handle wide variety of liquids including highly viscous liquids(< 100 mPa·s).

We propose a method to synthesize functional microparticles, by in-air composition of droplet emitted by inkjet. Since the viscous resistance in-air system is much smaller than that in microfluidic devices, this method has an advantage of generating microparticles at high rate. Moreover, the functional microparticles generated can be patterned in the same way as inkjet printing(Fig. 1).

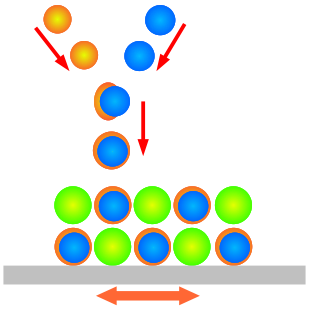

Figure 1: Synthesis and patterning of functional microparticles using inkjet technique.

2 EXPERIMENTAL EQUIPMENT

We developed a new liquid droplet emission system, equipped with microscopic observation with high temporal resolution observation system as high as 0.1 μs. Schematic view of the droplet ejection system is shown in Fig. 2. The inkjet equipment consists of a piezoelectric actuator and a glass capillary, of which inner radius of the orifice is 8, 15 and 30 μm. This equipment can handle wide variety of liquids, including strong acids, alkalies and viscous liquids of which viscosity is smaller than 20 mPa·s.

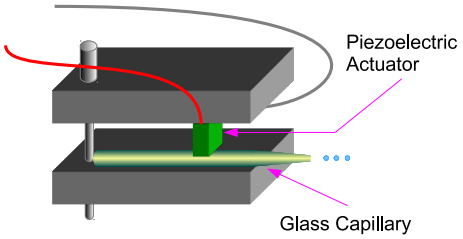

Figure 2: Schematic picture of inkjet equipment.

As mentioned above, the motion of the droplets have high reproducibility, we observed the droplets with a stroboscopic microscope. The timing of the droplet emission and the trigger of the strobe flash light are controlled by a function generator. We achieved the temporal resolution of 0.1 μs and the spatial resolution of 1 μm, which is higher than the commercially available high speed camera.

3 OBSERVATION OF DROP OSCILLATION

We observed the collision of droplets, emitted by facing two inkjet nozzles. The position of the nozzles are adjusted so that the total amount of rotational momentum of the fused droplet becomes zero. As shown in Fig. 3, the collided droplet oscillates with the surface tension as the force of restriction and damps to form an equilibrium shape by the viscoity.

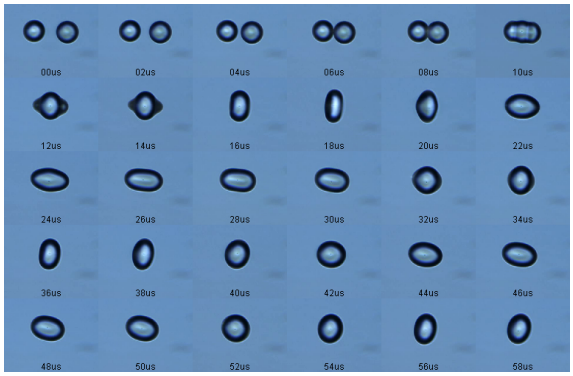

Figure 3: Collision and normal oscillation of pure water droplet with radius of 30 μm.

We observed the oscillation of several kinds of liquids, including water, silicone oils, surfactant solutions and associated liquids, and examined liquid properties.

In case the oscillation amplitude is small and the viscosity can be neglected, the oscillation in the shape of a free droplet dominated by the hydrodynamic and the displacement for the eigen oscillations are described in terms of the spherical harmonic function.

The eigen oscillation frequency of inviscid droplet at l-th mode is given by

$$\omega_l = \sqrt{l(l-1)(l+2)\sigma/\rho R^3} \tag{5}$$

where R is the radius of the equilibrium state, σ and ρ are liquid surface tension and density, respectively. This oscillation is damped by viscous dissipation, and the damping rate of the fundamental $l = 2$ mode can be calculated to

$$\gamma_{l=2} = 5\eta/\rho R^2, \tag{6}$$

where the oscillation frequency is sufficiently larger than the oscillation damping rate γ. From equations (5) and (6), the surface tension σ and viscosity η are obtained from the droplet oscillation frequency ω and damping rate γ independently.

The time variation of the droplet lengthwith respect to the polar and equatorial axis are shown in Fig. 4. From the figure we obtained the oscillation frequency ω and damping rate γ, and compared the experimentally obtained surface tension to the literature values. For pure liquids with relatively small viscosity, the experimental values of oscillation frequency is within 90-95 % of the theoretical value derived from the literature values of surface tension and viscosity. The discrepancy may be due to the nonlinear effect caused by large amplitude.

In addition, we analyzed the oscillation of droplets of surfactant solution. As shown in Fig. 4(c), the waveform of SDS solution droplet is apparently distorted from the harmonic form, which can be attributed to the surface absorption of surfactant molecules.

For liquids with larger viscosity, the effect of viscosity to the oscillation becomes large and the droplet mo-

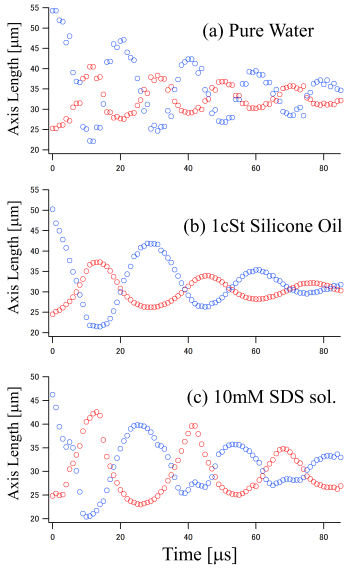

Figure 4: Normal oscillation of droplet of small viscosity.

tion is no longer the damped oscillation. The behavior of the droplets obtained for 20 cSt silicone oil droplet is shown in Fig. 5, where the overdamped oscillation is observed. We analyzed the asymptotic behavior of the

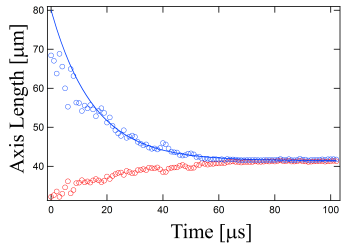

Figure 5: Overdamped oscillation of 20 cSt silicone oil droplet.

droplet motion and obtained the experimental value of the normalized viscosity ϵ which is defined by

$$\epsilon = \eta/\sqrt{\rho R\sigma}. \tag{7}$$

The asymptotic behavior of drop oscillation was described by [5],

$$\kappa^2 - 2\Gamma_{l0}\kappa + \Omega_{l0}^2 - 2(l-1)^2(l+1) \times \frac{2J_{l+3/2}(\xi)}{2J_{l+3/2}(\xi) - \xi J_{l+1/2}(\xi)}\epsilon\kappa = 0. \tag{8}$$

We define here the normalized complex frequency as $\kappa = (\rho R^3/\sigma)^{1/2}(\gamma + i\omega)$, constants $\Gamma_{l0} = (l-1)(2l+1)\epsilon$ and $\Omega_{l0} = l(l-1)(l+2)$.

Here, the complex frequency depends only on the normalized viscosity ϵ. The normalized frequency $\Omega = (\rho R^3/\sigma)^{1/2}\omega$ and damping rate $\Gamma = (\rho R^3/\sigma)^{1/2}\gamma$ are plotted against ϵ in Fig. 6.

For the low viscosity limit, eq.(8) is approximated to

$$\kappa^2 - 2\Gamma_{l0}\kappa + \Omega_{l0}^2 = 0, \tag{9}$$

which represents the damped oscillation with frequency $\sqrt{\omega_{l0}^2 - \gamma_{l0}^2}$ and damping rate γ_{l0}. This result is consistent with the inviscid limit.

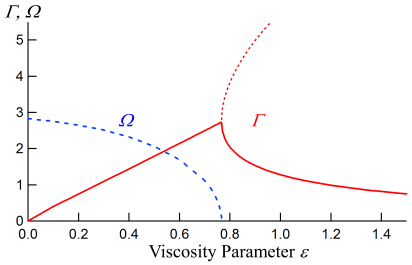

Figure 6: Normalized frequency and damping rate versus viscosity parameter ϵ calculated by eq.(8). The complex frequency has one real and one imaginary solutions for $\epsilon < 0.76$ and two real solutions for $\epsilon > 0.76$.

The experimental and literature values of the normalized viscosity ϵ are displayed in Fig. 7. This figure shows the correlation between the static and dynamic values of the shear viscosity. For water, silicone oils and glycerol solution, the experimental values agree well with the literature. However, for ethylene glycol and diethylene glycol, the experimental values are only about half of the static ones. This phenomena can be attributed to the slow viscous relaxation of associated liquids due to the re-combination dynamics of the H-bond network.

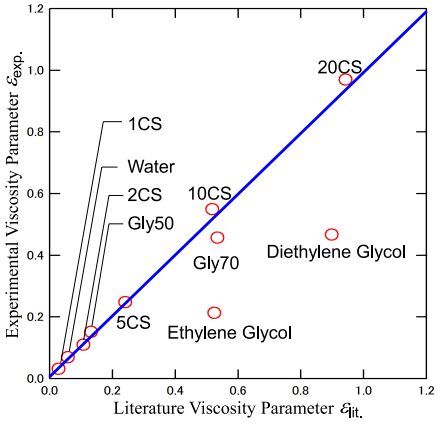

Figure 7: Comparison of experimental values of viscosity parameter $\epsilon_{\rm exp}$ and viscosity parameter obtained by literature values of liquid properties obtained at the static condition $\epsilon_{\rm lit}$.

4 OBSERVATION OF COMBINED DROPLET OF IMMISCIBLE LIQUIDS

When two immiscible droplets, such as oil and water, are in contact to each other, the equilibrium shape of the combined droplet is formed so as to minimize the total energy of surface and interface. The equilibrium shape is classified into two types: capsule and two-lobed, corresponding to the complete and the partial wet, respectively.

Since the balance between surface and interfacial tensions determines the equilibrium shape, we can determine the ratio between surface and interfacial properties from the shape. The experimental approach in macroscopic size has been suffered from the harm of the gravity that deforms the droplet from the ideal shape. In our microscopic experiment, the effect of the gravity is negligible and only the contribution of the surface and interfacial energy determines the droplet shape.

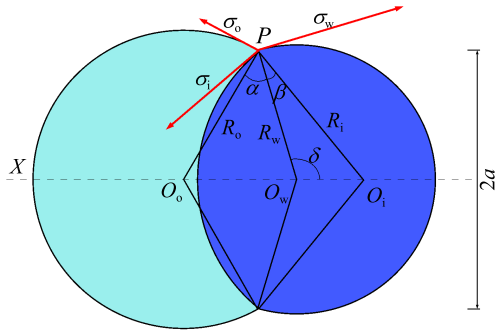

Figure 8: Schematic picture of oil-water combined droplet.

The schematic picture of combined droplet under partially wet condition is shown in Fig. 8. The axis X is the symmetrical center of the combined droplet and P indicates triple-line boundary of three media, such as water, oil and air. The notations $\vec{\sigma}_w, \vec{\sigma}_o$ and $\vec{\sigma}_i$ are vectors of water surface tension, oil surface tension and oil-water interfacial tension, respectively. The axis PO_w, PO_o and PO_i are perpendicular to the vectors $\vec{\sigma}_w, \vec{\sigma}_o$ and $\vec{\sigma}_i$ on triple-line P, and they cross with X at point O_w, O_o and O_i, which are the center of the curvature of water surface, oil surface and water-oil interface, respectively. The angle δ is taken between PO_w and X. This picture automatically satisfies the Young-Laplace equation of

$$\sigma_w H_w - \sigma_o H_o - \sigma_i H_i = 0, \tag{10}$$

and the balance of surface and interfacial tension vectors

$$\vec{\sigma}_w + \vec{\sigma}_o + \vec{\sigma}_i = 0. \tag{11}$$

From the picture, we can obtain the curvatures of the inner interface if volume ratio of oil and water droplet is known, therefore, we can calculate ratios between the surface and interfacial tensions from the experimental image of the combined droplets.

We observed the equilibrium shape of combined droplet of various oil/water volume ratio, and the experimental results are in harmony with the literature values(Fig. 9). This experiment provides high-speed and non-contact measurement of the surface and interfacial tension in microscale liquid.

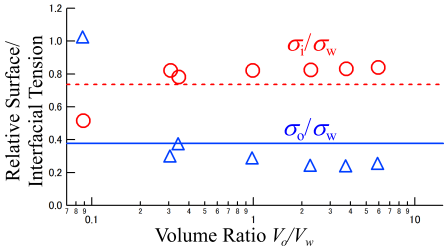

Figure 9: Relative surface and interfacial tension calculated by the equilibrium shape of hexadecane-water combined droplet.

5 CONCLUSION

We developed a new method to measure microscale liquid properties with extremely high temporal resolution, by observing the dynamics of a 10-micron droplet. These experiments will provide fundamental knowledges on the dynamics and properties of microscopic liquids, and contribute to the development of microscale liquid industry.

REFERENCES

[1] H. Lamb, "Hydrodynamics 6th ed.," Cambridge University Press, 1932.

[2] S. Chandrasekhar, "Hydrodynamic and Hydromagnetic Stability," Clarendon Press, 1961.

[3] O. A. Basaran, "Nonlinear oscillations of viscous liquid drops," J. Fluid Mech. 241, 169–198,1992.

[4] T. Yamada & K. Sakai, "Observation of collision and oscillation of microdroplets with extremely large shear deformation", Physics of Fluids 24, 022103, 2012.

[5] A. Prosperetti, "Normal-mode analysis for the oscillations of a viscous liquid drop in an immiscible fluid," J. Méc. 19, 149–182, 1980.

[6] H. Kutsuna & K. Sakai, "Hyper rheology measurement by emission and collision of micro-fluid particles," Appl. Phys. Express 1, 027002, 2008.